Sound sources in premixed flames

Mohsen Talei

Department of Mechanical Engineering, The University of Melbourne, Australia

Abstract

This paper presents a technical review of our understanding of the mechanism of sound generation by premixed flames. Examples from direct numerical simulation (DNS) studies undertaken at the University of Melbourne are provided. Furthermore, the implications of the findings for developing accurate models that can predict combustion-generated sound are discussed. This paper demonstrates that flame-flame interactions referred to as 'flame annihilation' are significant sources of sound in premixed flames. These localised events feature several unique characteristics that cannot be explained with existing turbulent flame theories. It is shown that flame acceleration during annihilation has a significant contribution to the radiated sound. Therefore, in the context of modelling, it is essential to predict the flame displacement speed during annihilation as accurately as possible. Analysis of the DNS data shows promising avenues to meet this requirement.

Keywords: combustion noise, premixed flames, flame annihilation

1. Introduction

One of the significant challenges we face in the 21st century is how to secure our demand for energy safely, efficiently and in an environmentally sustainable manner. This has driven a considerable effort to promote the widespread use of renewable energy and alternative fuels. Nevertheless, fossil fuels are still dominant in the energy market. The most optimistic scenario proposed by the International Energy Agency (IEA) predicts that we still rely on combustion of fossil fuels and biofuels for meeting 70% of our energy needs in 2040 [1]. This calls for further research to enhance our understanding of combustion process to advance energy-producing technologies that are cleaner and highly efficient.

Gas turbines are the prime movers in the aviation industry and account for about 20% of the installed capacity for electricity generation globally [2]. They have fast ramp up and down capabilities, which make them complementary to intermittent renewable generation. Furthermore, with the increasing interest in producing renewable hydrogen, gas turbines can play an important role in the implementation of a successful hydrogen economy.

Lean premixed combustion is the desired combustion regime in industrial gas turbines. It results in a low level of NO_X emissions due to operating at lower temperatures and facilitates better combustion efficiency. However, the primary issue with operating gas turbines in this regime is thermoacoustic instability, commonly initiated by combustion-generated sound. To avoid this type of instability, the mechanism of sound generation by premixed flames needs to be fully understood. Numerous theoretical, numerical, and experimental studies have explored this problem from various angles. An interested reader is referred to the review articles by Candel [3], Dowling and Mahmoudi [4] and Ihme [5].

To characterise combustion noise, many past studies have considered unconfined flames. They generally conclude that combustion noise features a broadband spectrum and that the sound spectra show some degree of universality in terms of the frequency of peak emission and the slope of the spectrum in the low and high frequency ranges. The experimental study by Rajaram et al. [6] is an example of a comprehensive experimental dataset of sound generation by premixed flames for different fuels, equivalence ratios and flow parameters. They show that the frequency of peak emission can be estimated as a function of the average flame length and burner diameter.

Another important observation in the literature is that the fluctuating heat release rate is an important source of noise [3]. Many past studies have demonstrated this and used a framework such as acoustic analogies to further analyse this problem. As demonstrated in the literature and discussed further in this paper, flame-flame interaction or flame annihilation is a significant source of heat release rate fluctuations.

Numerical simulation is a tool that can provide a further understanding of this problem. Amongst different numerical approaches, direct numerical simulation (DNS) is a promising tool due to its ability to resolve all length and time scales in the problem. This paper therefore aims to review the DNS studies in this regard, primarily undertaken at the University of Melbourne. It will be shown how DNS can provide unprecedented detail about the source of sound in premixed flames and how this information can be used for developing new models that can predict sound generation by premixed flames for practical problems.

2. Acoustic Analogy

Acoustic analogies have been extensively used to study the mechanism of sound generation by different types of flows. In general, they are a rearrangement of the Navier-Stokes equations into various forms of an inhomogeneous wave equation. The source terms on the right hand side of acoustic analogies can then be used to interpret the sound generation mechanism. Lighthill [7,8] proposed the first and best known acoustic analogy by rearranging the continuity and momentum conservation equations into a wave equation. This equation was reformulated by Dowling [9] to examine sound generation by combusting flows,

$$\frac{1}{c_\infty^2}\frac{\partial^2 p}{\partial t^2} - \nabla^2 p = \frac{\partial}{\partial t}\left(\frac{\rho_\infty}{\rho}\left(\frac{Q\dot{\omega}}{c_p T} - \frac{\nabla \cdot \boldsymbol{q}}{c_p T} + \frac{\tau_{ij}}{c_p T}\frac{\partial u_i}{\partial x_j}\right)\right)$$
$$+ \frac{\partial^2}{\partial x_i \partial x_j}\left(\rho u_i u_j - \tau_{ij}\right)$$
$$+ \frac{1}{c_\infty^2}\frac{\partial}{\partial t}\left(\left(1 - \frac{\rho_\infty c_\infty^2}{\rho c^2}\right)\frac{Dp}{Dt} - \frac{p - p_\infty}{\rho}\frac{D\rho}{Dt}\right)$$
$$+ \frac{\partial^2}{\partial x_i \partial t}(u_i \rho_e).$$
$$(1)$$

where p is the pressure, T is the temperature, c is the speed of sound, Q is the heat of combustion, $\dot{\omega}$ is the reaction rate, ρ is the density, c_p is the specific heat capacity, $\boldsymbol{q}$ is the heat flux, τ_{ij} is the viscous stress tensor, u is the velocity, x is the spatial coordinates and t is the time. The subscript ∞ refers to the flow field variables in the far field. Here ρ_e is the excess density, defined as,

$$\rho_e = \rho - \rho_\infty - (p - p_\infty)/c_\infty^2. \quad (2)$$

The first line on the right hand side of Equation 1 is a monopolar source term which is considered to be the main contributor to combustion noise. The second line is the so-called Lighthill's stress tensor which is a dominant source of sound in non-reacting jets. As discussed by Dowling [9], the source term in the third line is significant if there are regions of unsteady flow with different mean density and sound velocity from the ambient. The last term is a dipole source due to changes in the momentum of density inhomogeneities. Considering the first term on the right hand side of Dowling's formulation as the only source term, leads to:

$$\frac{1}{c_\infty^2}\frac{\partial^2 p}{\partial t^2} - \nabla^2 p = \frac{\partial}{\partial t}\left(\frac{\rho_\infty}{\rho}\left(\frac{Q\dot{\omega}}{c_p T}\right)\right). \quad (3)$$

Equation 3 is used in several combustion noise studies to obtain the far-field sound using Green's function solution and study the mechanism of sound generation. However, there is evidence in the literature that other source terms, such as the last source term in equation 1 can play an important role under some circumstances [10-11]. This review will demonstrate the range of validity of equation 3 under some conditions.

3. Numerical methods

3.1 Numerical solvers

Two DNS solvers were used to study sound generation by premixed flames. The first solver is NTMIX, developed at the European Center for Research and Advanced Training in Scientific Computing (CERFACS). NTMIX features a sixth-order compact scheme for spatial derivatives, combined with a third-order Runge–Kutta time integrator [12]. This solver uses a simple chemistry model and has been used extensively to study laminar and turbulent flames. The second DNS solver is S3D_SC [13] which is a modified version of S3D [14], a solver originally developed at the Combustion Research Facility at Sandia National Laboratories. This solver features an eighth-order central differencing scheme for spatial derivatives, combined with a six-stage, fourth-order explicit Runge–Kutta time integrator.

3.2 Computational domains and numerical parameters

3.2.1 Laminar flames

Two groups of configurations are considered here. The first group includes one-dimensional (1D) domains for simulating planar, axisymmetric and spherically symmetric annihilation events. Figure 1 shows a schematic of these configurations. Figure 1a shows the configuration for a planar flame annihilation and half of the domain is considered by using a symmetry line on the left hand side. The outflow boundary is located on the right hand side. The flame is initialised in the middle of the domain with the unburnt gas trapped between the flame and the symmetry line. As a result of this initialisation, the flame propagates towards the symmetry line until it annihilates. Figure 1b shows the configuration for axisymmetric and spherically symmetric annihilation events. For these cases, spherical and cylindrical flames are initialised at a given radius with the unburnt gas trapped inside them. The flame therefore propagates toward the origin until it completely collapses.

The second group consists of a two-dimensional (2D) laminar flame, forced at the inlet for a range of frequencies (see Figure 1c). The boundary conditions are imposed at the inflow, while non-reflecting boundary conditions are used at the outflow boundaries. For the baseline case (i.e. 1D planar), the temperature ratio T_b/T_u is considered to be 4, the Zel'dovich number β is 8, the non-dimensional laminar flame speed S_L/c_∞ is 0.01, the Lewis number is unity and the Prandtl number is 0.75. More details of the simulation and computational domain parameters can be found in [15,16].

3.2.2 Turbulent flames

Figure 3 shows a schematic of the computational domain for the turbulent flames considered. In these cases, turbulent premixed flames at two equivalence ratios of 0.7 and 1 were considered. A careful treatment of boundary conditions was undertaken to avoid spurious noise at the boundaries. For instance, a sponge layer at the outflow was considered to avoid reflection from the outflow boundary. The jet Reynolds number was 5300 and the inlet Mach number was 0.35. More details of the simulation and computational domain parameters can be found in [18].
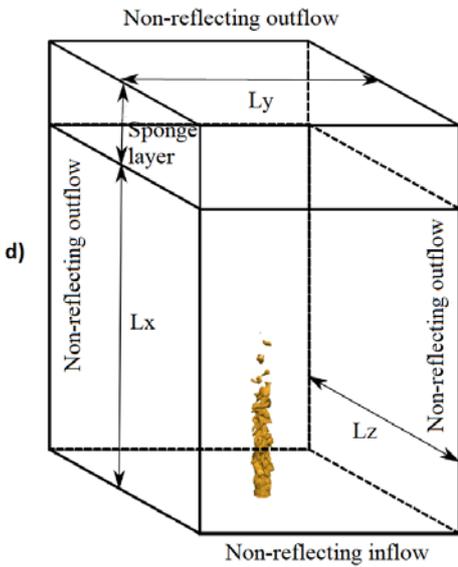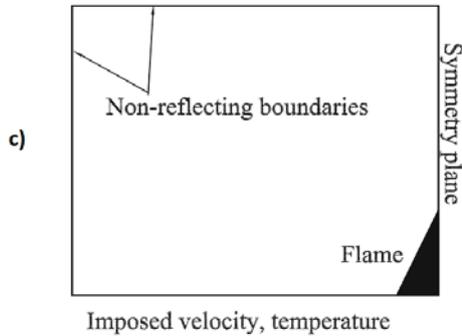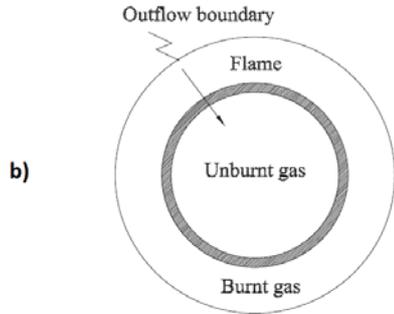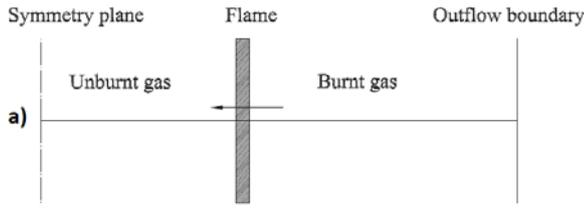
Figure 1: *Computational domains for a) planar, b) axisymmetric and spherically symmetric annihilation, c) acoustically forced premixed flame and d) turbulent premixed flame.*

4.   Results

Annihilation events are a significant source of heat release rate fluctuations. To understand the mechanism of sound generation by these events, simple geometries including planar, axisymmetric and spherically symmetric cases will be first examined in this section [15,16]. Using the theoretical framework discussed in section 3, the proposed scaling laws to estimate sound generation by these events will be reviewed [15]. Using these scaling laws and DNS results, the impact of the key flame parameters such as flame thickness, laminar flame speed, temperature ratio, Zel'dovich number and Lewis number on the produced sound will be discussed [16]. Next, the significance of these events in 2D forced laminar flames will be investigated [17]. This follows by reporting a 3D DNS of sound generation by turbulent premixed flames [18]. An algorithm for identifying annihilation events will be presented and the contribution of these events to the overall produced sound will be quantified [19]. Finally, the implications of these results for modelling will be discussed [20].

4.1 Sound generation by 1D flame annihilation

4.1.1. Planar flame annihilation

Figure 2 shows pressure and heat release rate profiles for several instants before, during and after flame annihilation in the planar configuration discussed in section 3 (see Figure 1a). The top row shows the reaction rate as a function of distance, featuring a flame propagating towards the unburnt mixture. As can be seen, when the flame is approaching the symmetry line, the peak reaction rate slightly increases. This increase correlates with a pressure rise at the symmetry line shown in the bottom row of Figure 2. After annihilation, a pressure wave with a large negative amplitude propagates towards the outflow. As the wave propagates at the speed of sound in the burnt region, this negative amplitude remains constant (not shown here for brevity).
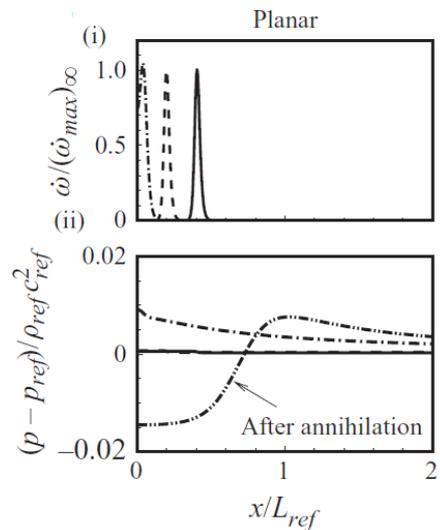

Figure 2: *(i) Normalised reaction rate and ii) pressure fluctuations before (solid, dashed), during (dash-dotted) and after flame annihilation (dash dot-dot).*
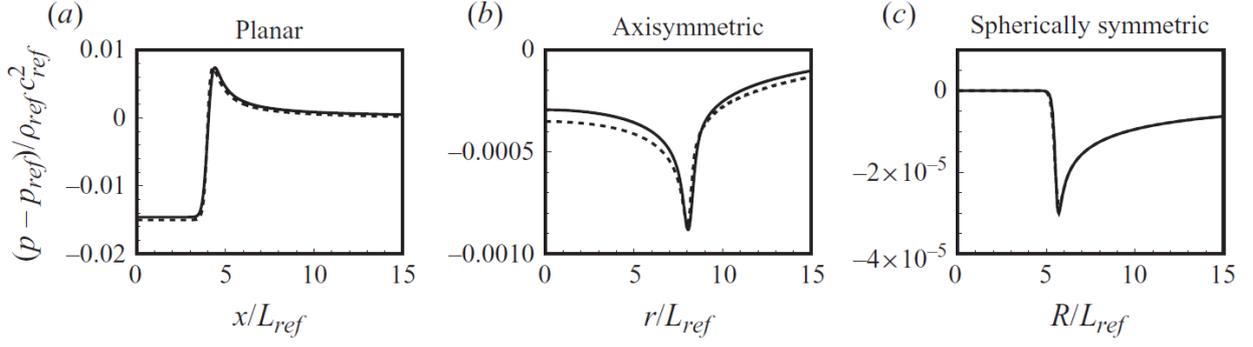
Figure 3: *Comparison of the far-field pressure fluctuations from the DNS (solid line) and the solution of equation 3 (dashed line) for a) planar, b) axisymmetric and c) spherically symmetric annihilation.*

4.1.2. Axisymmetric and spherically symmetric flame annihilation

For the axisymmetric and spherically symmetric annihilation events, the pressure wave produced by these events are shown in Figure 3. These pressure waves only feature negative values. In order to understand the source of these pressure waves, equation 3 is solved for these simple configurations using free-space Green's functions. There is a good agreement between this solution and the DNS results, confirming the dominance of the heat release rate fluctuations as a source of sound. Since annihilation events are responsible for destruction of the flame surface area, i.e. negative fluctuations of the heat release rate, it is expected to observe negative pressure fluctuations as a result.

4.1.3. Scaling laws

In this section, a scaling law will be presented to investigate the mechanism of sound generation by annihilation events. Using the analytical solution of equation 3 for all types of annihilation events with their corresponding Green's functions, a scaling law can be obtained to relate the generated sound p' to key flame parameters [15,16]:

$$\frac{p'}{\rho_u c_u^2} = \left(\frac{S_L}{c_u}\right)^{1+\frac{n}{2}} \left(\frac{\delta}{\zeta}\right)^{\frac{n}{2}} \left(1 - \frac{T_u}{T_b}\right) \left(\frac{T_b}{T_u}\right)^{\frac{2-n}{4}} g\left(\frac{T_b}{T_u}, \beta, Le, \zeta, t\right) \quad (4)$$

where n = 0 for planar, 1 for axisymmetric and 2 for spherically symmetric annihilation events. The variable δ is the flame thickness, ζ is the distance between the observer and the origin, $\frac{T_b}{T_u}$ is the temperature ratio, β is the Zel'dovich number and *Le* is the Lewis number.

Equation 4 explains how different configurations affect the radiated sound. While the flame thickness does not play a role for planar annihilation, it becomes an increasingly important parameter when the configuration changes from axisymmetric to spherically symmetric. This scaling shows that thicker flames will produce more sound when n=1 and 2. The dependency on S_L also becomes stronger as we move from planar to spherically symmetric annihilation. One should also note that the proposed scaling cannot fully explain the importance of parameters such as temperature ratio, Zel'dovich number and Lewis number as all shown as parameters in the unknown function *g*. This motivated a separate DNS study, discussed in section 4.1.4.

4.1.4. Effects of key flame parameters on sound generation

In a series of DNS studies, the effects of parameters such as flame thickness, laminar flame speed, Zel'dovich number, temperature ratio and Lewis number on the generated sound by annihilation events were investigated [16]. Consistent results with the proposed scaling was generally observed. Amongst different parameters, the impact of Lewis number was particularly of interest. Three cases with the Lewis numbers of 0.5, 1 and 2 were considered. For the Le=2 case, a similar behaviour to the Le=1 case was observed except for a higher peak amplitude of the heat release rate during annihilation for the Le=2 case. This led to generation of a pressure wave featuring a large positive peak as well as the same negative pressure amplitude as the Le=1 case. This is linked to the fact that the preheat layer is thicker than the mass diffusion layer for Le=2, leading to the merging of the preheat layers at the initial stage of annihilation and therefore, providing additional heat. This then causes a higher peak amplitude for the heat release right before annihilation. For the Le= 0.5 case, the mass diffusion layer is thicker. As a result, during annihilation, the unburnt gases are depleted and the flame is extinguished before it reaches the symmetry line. This process is relatively slow and therefore leads to generation of a pressure wave that has a large wavelength but the same negative pressure amplitude as the Le = 1 and 2 cases.

Figure 4 : Non-dimensional temperature fields at St = 1 (left column), St = 0.1 (middle column) and St = 0.025 (right column) of the perturbed flame at several instants during a forcing cycle. The Strouhal number is defined here as $St = fL_{ref}/c_{ref}$ where L_{ref} is half of the inlet width and c_{ref} is the speed of sound at the inlet.
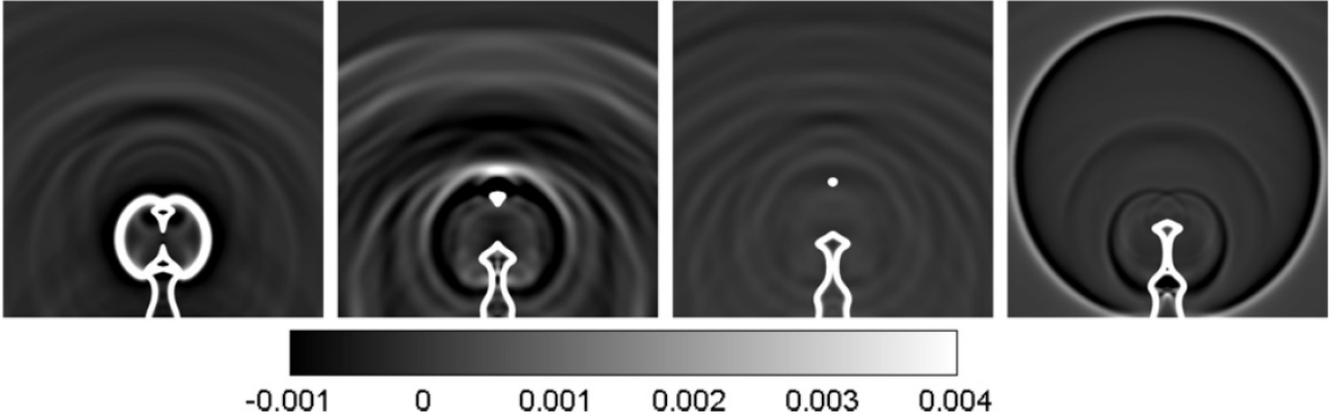

Figure 5: Dimensionless dilatation ($\nabla . \boldsymbol{u}$) field for the St=0.025 case for several instants during a forcing cycle.

4.1.5. The importance of displacement speed

In a series of DNS and theoretical studies, the flame displacement speed was identified as a key parameter contributing to the radiated sound [15,16]. An example of a theoretical study is provided here. Considering the reaction rate as a delta-function with a constant consumption speed, i.e.,

$$\dot{\omega} = \rho_u S_L \delta\big(\zeta_f(\tau) - \zeta\big), (5)$$

where ζ_f is the instantaneous flame location and ζ is the spatial coordinates, the pressure fluctuations in the far field can be described using the Green's function solution of equation 3. The solution for a spherically symmetric annihilation event is only expressed for brevity:

$$p'(R,t) = -2\rho_u S_L \left(1 - \frac{T_u}{T_b}\right) \times$$
$$\zeta_f(t - R/c_b)V_f(t - R/c_b)H(t - R/c_b), \quad (6)$$

where V_f is the flame propagation velocity, R is the flame radius and H is a Heaviside step function. The flame propagation speed V_f can be described as a function of the gas velocity and the flame displacement speed:

$$V_f = u + S_d. \quad (7)$$

During annihilation, the flame experiences a large variation of S_d, therefore contributing to sound generation. The displacement speed can also be used as a marker to identify annihilation events as will be discussed in section 4.3.

4.2 Sound generation by 2D laminar flames

To further investigate the mechanism of sound generation in premixed flames, acoustically forced 2D flames are now considered. These flames are perturbed by imposing velocity fluctuations at the inflow. Figure 4 shows the instantaneous temperature fields for three forcing frequencies. The flame does not respond at the highest forcing frequency, corresponding to short acoustic wavelengths. As the forcing frequency decreases, increased flame wrinkling is observed, and a disturbance propagates along the flame surface at the convective wavelength U_{in}/f where U_{in} is the mean flow velocity. For the lowest forcing frequency, a high degree of wrinkling is observed. At some stage during the forcing period, this forms an elongated flame leading to a 'flame pinch-off' event, as a result of which a pocket of unburnt reactants is detached from the flame. This pocket is gradually consumed as it convects further downstream. The consumption of this pocket is referred to as an 'island burn-out' event.

Figure 5 shows the dilatation ($\nabla . \boldsymbol{u}$) field at instants during one period of excitation for the *St = 0.025* case. The dilatation is commonly used in aero-acoustic studies to identify sound, as pressure and dilatation are related for small Mach number flows. In the present study, the dilatation has the added property that it simultaneously shows the flame as well as the generated sound. It can be observed that the flame pinch-off and island burn-out events are strong sources of sound. The flame pinch-off event can be considered as a planar like annihilation event whereas the island burn out is analogous to an axisymmetric annihilation
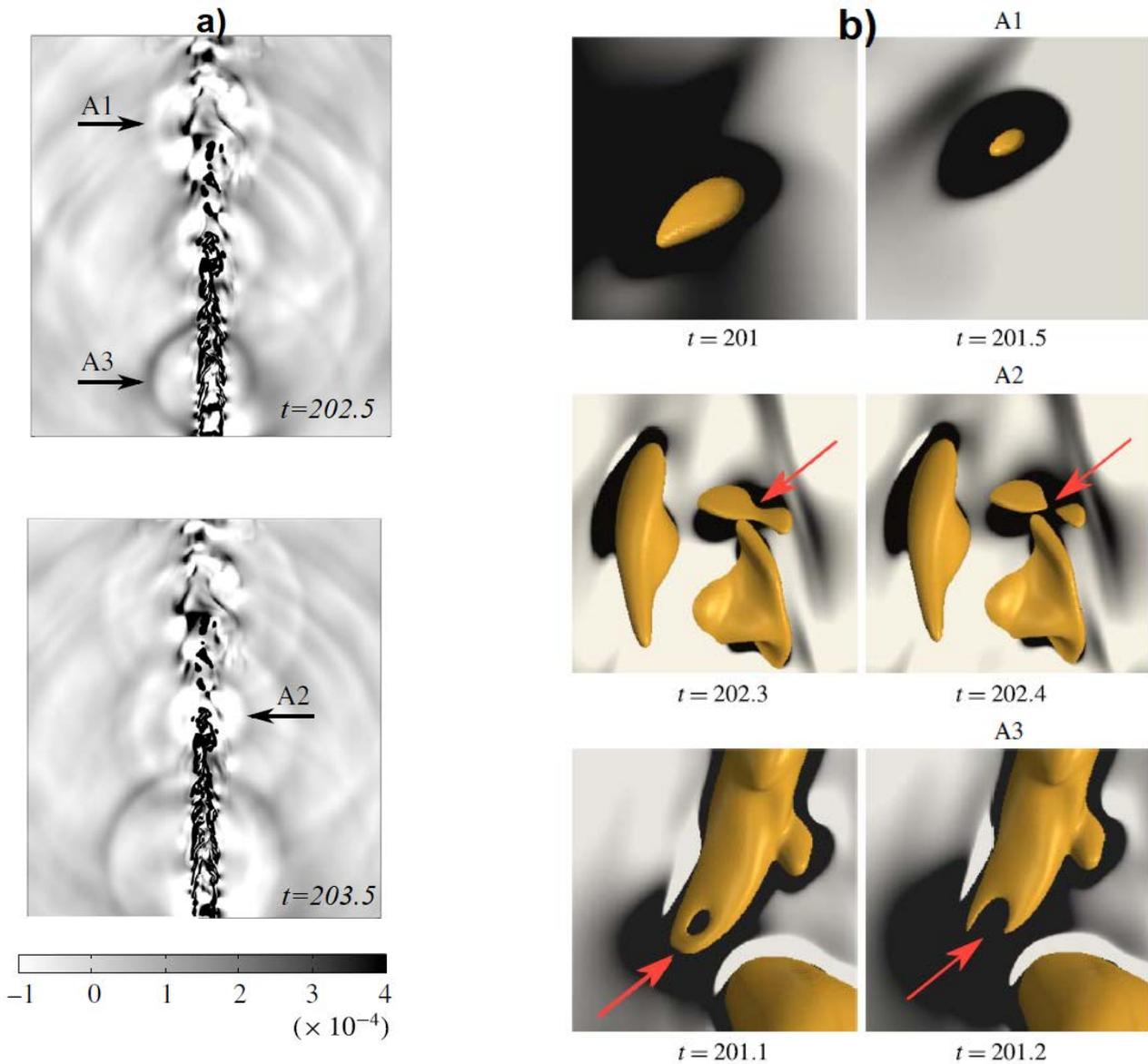
Figure 6: a) Dimensionless dilatation field for the φ=1 case and b) iso-surface of progress variable superimposed on the dilatation field for the selected events A1-A3.

event both of which studied earlier in detail [15,16]. The next question is whether annihilation events are significant noise sources in turbulent premixed flames. This motived the DNS study discussed in section 4.3.

4.3 Sound generation by turbulent flames

Sound generation by 3D turbulent flames described in section 3.2.2. is now examined. An instantaneous snapshot of the dimensionless dilatation field on the central x–y plane through the jet is shown for the φ=1 case in Figure 6a. The presence of numerous spherical acoustic waves suggest that the acoustic field is dominated by monopolar noise sources. To further examine these sources, three events resulting in pressure waves shown with A1, A2 and A3 in the dilatation field are selected.

Figure 6b shows a flame iso-surface of progress variable for events A1, A2 and A3 in figure 3 superimposed on the dilatation field. The selected iso-surface corresponds to the point of the peak heat release in a one-dimensional premixed

flame with the same chemistry. The event A1 involves the consumption of a pocket of unburned gases in the downstream region near the flame tip. Consistent with our earlier studies [17], this phenomenon is referred to as 'flame island burn out'. Event A2 is referred to as a 'flame pinch-off', with a pocket of unburned gases detaching from the flame surface. Finally, the event A3 takes place when flame-to-flame interaction first results in the formation of a tunnel of burned gas, and then the local flame area is lost due to cusp retraction associated with another pinch-off event. This first event is called 'tunnel formation'. Figures 6b together with the results shown in figure 6a suggest that these frequent flame annihilation events play an important role in the generation of sound.

To accurately quantify the contribution of these events to the overall radiated sound by the flame, annihilation events were identified in a separate work by finding the critical points in the progress variable field [19]. An algorithm was developed to find these events in an automated process and track their position such that their individual contribution can be

$$\frac{S_d}{S_L} = 1 - Ma\,Ka, \quad (8)$$

where Ma is the Markstein number and,

$$Ka = \frac{\delta}{S_L}\big(a_T + Sd(\boldsymbol{\nabla}.\boldsymbol{n})\big). \quad (9)$$

The variable a_T is the tangential strain rate and $\boldsymbol{n} = \frac{\boldsymbol{\nabla}Y}{|\boldsymbol{\nabla}Y|}$ where Y is the progress variable.

This theory is particularly relevant for a level-set type combustion model where the evolution of the flame surface is the phenomenon of interest:

$$\rho\frac{\partial G}{\partial t} + \rho u_i \frac{\partial G}{\partial x_i} = \rho_0 S_d |\nabla G| \quad (10)$$

where G represents the flame front and ρ_0 is the fresh gas density. As can be seen, a correct estimation of S_d as a function of the local properties such as curvature and strain rate is an important part of this model.

As discussed in section 4.1.5., the displacement speed plays an important role in the generation of sound by annihilation events. To investigate whether Markstein theory is applicable for estimation of S_d, a joint PDF of S_d^*/S_L and Ka is shown in Figure 8. Note that $S_d^* = \rho S_d/\rho_u$. The iso-surface of the progress variable corresponding to the maximum reaction rate is chosen to collect the data. First, the entire flame surface is considered. As can be seen, there is a strong correlation between the displacement speed and Karlovtiz number. The joint PDF for annihilation events identified by the points on the surface featuring $S_d^*/S_L > 5$ is shown in Figure 8b. A stronger correlation between the displacement speed and Karlovitz number is observed for these events. Least-squares fitting over the DNS data showed that a modified Markstein number referred to as *annihilation* Markstein number can reasonably describe the dynamics of annihilation events. This number was in agreement with that calculated by averaging the Markstein numbers of axisymmetric and spherically symmetric annihilation events under the same conditions as the turbulent flames.

5.   Future work

The analyses presented for annihilation events showed that these events need special attention in terms of modelling. This is particularly important for large-eddy simulation (LES) of sound generation by premixed flames. The future work will therefore focus on developing combustion models for annihilation events using *a priori* and *a posteriori* analyses of the DNS data. This will provide grounds for testing these models under more realistic conditions (e.g. more relevant Reynolds numbers) obtained in experimental setups. As discussed in section 1, sound generation plays a key role in initiating thermoacoustic instability and therefore the ultimate goal is developing more accurate models that
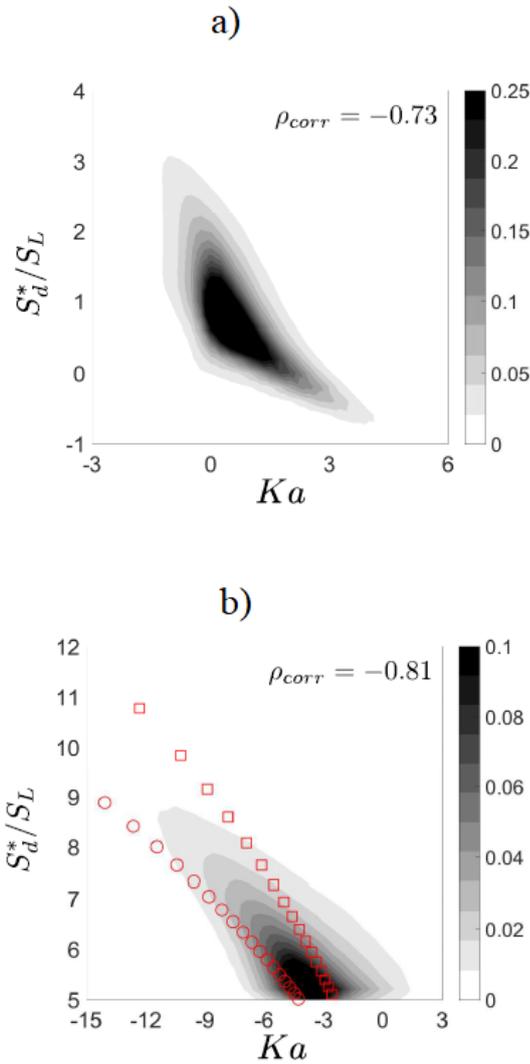

Figure 7*: A snapshot of the flame with the identified annihilation events using the critical points in the progress variable field. The two iso-surfaces represent the progress variable range used in the searching algorithm.*

determined. The technique also allowed the categorisation of these events based on their topologies. In addition to the previously found topologies, i.e. tunnel formation, pinch-off and island burn out events, a new type referred to as multi-feature event was identified. In this type, a combination of 2 or 3 events from the first group occurs in the vicinity of each other such that they cannot be categorised as an individual event (see Figure 7).

Two important observations were made in this study. First, different topologies are very similar in terms of the magnitude of the pressure fluctuations as well as the duration of the pressure wave. The second observation was related to the contribution of these events to the far-field sound. It was shown that the high frequency side of the sound spectrum (St > 1, where $St = fD/U_{in}$) can be fully explained by these events while they are not the main sound source but still important on the low frequency side. This suggests appropriate models for these short time scale events need to be developed such that the overall sound generated by premixed flames can be predicted accurately.

4.4 Implications for modelling

Markstein theory has been extensively used to study the variation of displacement speed as a function of curvature or Karlovitz number Ka for unsteady flames:

a)

b)

Figure 8: *Correlation of the normalised stretch (Ka) with S_d^*/S_L for $\varphi=1.0$ for a) the entire flame surface and b) considering only the annihilation events.*

can be used to predict thermoacoustic instability in gas turbines.

6.   Conclusions

This paper presented a technical review of our understanding of the mechanism of sound generation by premixed flames. Examples from the work undertaken at the University of Melbourne, mainly focused on direct numerical simulation (DNS) were provided. First, annihilation events as a significant source of heat release rate fluctuations and therefore sound generation were considered. To understand the mechanism of sound generation by these events, simple geometries including planar, axisymmetric and spherically symmetric annihilation events were examined. Scaling laws were proposed to estimate sound generation by these events . Then, the effect of key flame parameters such as flame thickness, laminar flame speed, temperature ratio, Zel'dovich number and Lewis number on the generated sound were investigated. Next, the significance of these events in 2D forced laminar flames and 3D turbulent

premixed flames was examined. An algorithm for identifying annihilation events was presented and the contribution of these events to the overall produced sound was shown to be significant, particularly on the high frequency side of the far-field pressure spectrum.

Furthermore, the implications of our findings for developing accurate models that can predict combustion-generated sound were discussed. It was shown that acceleration of the flame surface during annihilation has a significant contribution to the sound radiated by these events. Therefore, in the context of modelling, it is essential to model the annihilation process carefully. Analysis of the DNS data showed promising avenues to meet this requirement.

8.   References

[1] World Energy Outlook 2018, International Energy Agency, 2018.
[2] Global Power Plant Database, http://datasets.wri.org/dataset/globalpowerplantdatabase (12/10/2019).
[3] S. Candel; D. Durox; S. Ducruix; A.-L. Birbaud; N. Noiray; T. Schuller, Int. J. Aeroacoust. 8 (1) (2009) 1-56.
[4] A. P. Dowling, Y. Mahmoudi, *Proc. Combust. Inst.* **35** (2015) 65–100.
[5] M. Ihme , A*nnu. Rev. Fluid Mech.* **49** (2017) 227–310 .
[6] R. Rajaram , T. Lieuwen , Acoustic radiation from turbulent premixed flames, *J. Fluid Mech.* **637** (2009) 357–38
[7] M.J. Lighthill, *Proc. R. Soc. London* **211** (1951) 564–587.
[8] M.J. Lighthill, *Proc. R. Soc. London* **222** (1954) 1–31
[9] A.P. Dowling, *Modern Methods in Analytical Acoustics*, Springer (pp. 378–403).
[10] Brear M.J., Nicoud F., Talei M., Hawkes E. R., Giauque A., *J. of Fluid Mechanics*, **707**, (2012) 53-73.
[11] Talei, M., Brear M. J., Hawkes E. R., *Theor. Comp. Fluid Dyn.* **28** (2014) 385-408.
[12] B. Cuenot, B. Bedet, A. Corjon, *NTMIX3D user's guide manual* (1997) CERFACS.
[13] J.H. Chen et al. *Comput. Sci. Disc.* 2 (2009) 015001.
[14] S. Karami , E.R. Hawkes , M. Talei , J.H. Chen *J. Fluid Mech.* 777 (2015) 633–689.
[15] Talei, M., Brear, M.J., Hawkes, E.R., *J. Fluid Mech.* **679** (2011) 194-218.
[16] M. Talei , M.J. Brear , E.R. Hawkes, *Combust. Flame* **159** (2012) 757–769.
[17] Talei, M., Brear, M.J., Hawkes, E.R., *Proc. Combust. Inst.* **34** (2013) 1093-1100.
[18] A. Haghiri, M. Talei, M.J. Brear, E.R. Hawkes, *J. Fluid Mech.* **843** (2018) 29-52.
[19] D. Brouzet, A. Haghiri, M. Talei, M.J. Brear, *Combust. Flame* **204** (2019) 268–277.
[20] A. Haghiri, M. Talei, M.J. Brear, E.R. Hawkes, to appear in *Flow, Turb. Combust.* (2019).